Computational Fluid Dynamics Analysis of Lateral Striate Arteries in Acute Ischemic Stroke Using 7T High-resolution Magnetic Resonance Angiography

Futoshi Mori, PhD,* Fujimaro Ishida, MD, PhD,§ Tatsunori Natori, MD, PhD,† Haruna Miyazawa, MD, PhD,† Hiroyuki Kameda, MD, PhD,‖ Taisuke Harada, MD, PhD,‖ Kunihiro Yoshioka, MD, PhD,‡ Fumio Yamashita, PhD,* Ikuko Uwano, PhD,* Kenji Ito, PhD,* and Makoto Sasaki, MD, PhD*

Background: Infarcts in the lateral striate artery (LSA) territory can be caused by several pathological changes, including lipohyalinosis and microatheroma. However, fluid dynamic effects on these changes remain unknown. Thus, we investigated whether the fluid dynamic metrics of the LSAs were altered in patients with acute ischemic stroke using computational fluid dynamics (CFD) analysis. *Methods:* Fifty-one patients with acute ischemic stroke confined in the basal ganglia and/or corona radiata underwent high-resolution magnetic resonance angiography (HR-MRA) at 7T. We performed CFD analyses to obtain indices including the wall shear stress (WSS), WSS gradient (WSSG), and flow velocity (FV) and compared these values between the ipsilesional and contralesional sides in the patients with infarcts in the LSA or non-LSA territories. *Results:* In patients with LSA-territory infarcts, the WSS, WSSG, and FV values were significantly lower in the ipsilesional LSAs than in the contralesional LSAs (P = .01-.03), while these values in the proximal middle cerebral arteries showed no significant lateralities. In contrast, in patients with non-LSA-territory infarcts, there were no significant lateralities in the metrics between the ipsilesional and contralesional sides. *Conclusions:* The CFD analyses using HR-MRA revealed significantly low WSS and WSSG values of the ipsilesional LSAs compared with that of the contralesional side in patients with LSA-territory infarcts, suggesting that fluid dynamic factors of LSAs can be one of the risk factors for LSA-territory infarctions.

Key Words: Lateral striate artery—computational fluid dynamics—ultrahigh field—magnetic resonance angiography—acute stroke

From the *Division of Ultrahigh Field MRI, Institute for Biomedical Sciences, Iwate Medical University, Iwate Prefecture, Japan; †Department of Neurology and Gerontology, Iwate Medical University, Iwate Prefecture, Japan; ‡Department of Radiology, Iwate Medical University, Iwate Prefecture, Japan; §Department of Neurosurgery, Mie Chuo Medical Center, Mie Prefecture, Japan; and ‖Department of Diagnostic and Interventional Radiology, Hokkaido University Hospital, Japan.

Received May 9, 2019; revision received July 22, 2019; accepted July 30, 2019.

Financial Disclosure: This work was supported by JSPS KAKENHI (JP26461836), a MEXT Grant-in-Aid for Strategic Medical Science Research (S1491001), and MEXT-Supported Program for Research Branding Project (H29-A3).

Address correspondence to Futoshi Mori, PhD, Division of Ultra-high Field MRI, Institute for Biomedical Sciences, Iwate Medical University. 1-1-1 Idaidori, Yahaba-cho, Shiwa-gun, Iwate Prefecture 028-3694, Japan. E-mail: fumori@iwate-med.ac.jp.

1052-3057/$ - see front matter

https://doi.org/10.1016/j.jstrokecerebrovasdis.2019.104339

Introduction

The lateral striate artery (LSA), a perforating artery mainly originating from the horizontal part of the middle cerebral artery (M1), is one of the arteries responsible for ischemic stroke in the basal ganglia and corona radiata. Cerebral infarcts including these areas can be caused by various pathological processes, such as cardioembolism, large-artery atherosclerosis, and small-vessel occlusion (lacune).[1] In particular, the infarcts confined within the LSA territory are considered to be attributed to steno-occlusive changes of the LSAs due to lipohyalinosis or microatheroma.[2,3] LSAs are small in size with a diameter of .1-1.4 mm (mean, .5 mm)[4] so that digital subtraction angiography has been most commonly used to assess these changes,[5] because less invasive imaging modalities, like magnetic resonance (MR) imaging, can barely detect LSAs.

A recent advancement of ultrahigh-field 7T MR systems enable noninvasive visualization of perforating arteries including LSAs when using high-resolution magnetic resonance angiography (HR-MRA).[6,7] The HR-MRA at 7T provided precise information of LSA characteristics,[6,7] and revealed that morphological changes such as a decreased number of LSA stems and/or branches could occur in patients with hypertension or chronic stroke.[6,7] However, no studies have highlighted functional characteristics of the LSAs, including fluid dynamics properties, in patients with LSA-territorial infarcts.

Recently, computational fluid dynamics (CFD) analysis has been applied to elucidate rheological conditions to induce vascular wall lesions.[8-11] Studies using the CFD analyses revealed that the wall shear stress (WSS) and/or related metrics were significantly related to atherosclerotic changes in intracranial major arteries as well as the evolution and rupture of cerebral aneurysms.[8,12] However, hydrodynamic effects on the perforating arteries such as LSAs remain unknown. Thus, in this study, we evaluated whether any characteristics in fluid dynamics are associated with the LSAs of patients with LSA-territorial infarcts when using HR-MRA at 7T and CFD analysis.

Materials and Methods

Subjects

From October 2012 to June 2017, we prospectively enrolled 51 patients (36 men and 15 women; 37-82 years [median, 66 years]; infarct side, 32 left and 19 right) with acute ischemic stroke confined in the basal ganglia and/or corona radiata on the baseline MR images. We excluded those who were candidates for reperfusion therapies, had stroke due to steno-occlusive lesions of major cervical/intracranial arteries, embolism, vasculitis, arterial dissection, moyamoya disease, and those with contraindications for a MR examination. The neurological findings on admission included hemiplegia in 40 patients, sensory disturbance in 7, dysarthria in 26, and ataxia in 6 with a National Institute of Health Stroke Scale rating of 0-8 [median, 3]. Patient characteristics before hospitalization included hypertension in 32 patients, diabetes mellitus in 13, and dyslipidemia in 28. All patients received standard medical treatments, which included antiplatelet therapy, anticoagulants, neuroprotection, and transfusion. The study was performed after obtaining an approval from the institutional ethical committee (H24-68) and written informed consent from each patient.

Imaging Protocol

All subjects underwent MR examination using a 7T scanner (Discovery MR950, GE Healthcare, Waukesha, WI) with a quadrature transmission and 32-channel receive head coil unit within 3 weeks after stroke onset. We obtained 3-dimensional (3D) time-of-flight HR-MRA, in which the circle of Willis and LSAs were included, using a spoiled gradient-echo sequence with the following scanning parameters: repetition time, 14 milliseconds; echo time; 3.4 millisecond; flip angle, 15°; field of view, 12 cm; matrix size, 512 × 320; slice thickness, .6 mm; number of slices, 192; reconstruction voxel size, .23 × .23 × .30 mm after zero-fill interpolation; number of excitations, 2; and acquisition time, 16 minutes 04 seconds. In addition, diffusion-weighted images with b-values of 1000 s/mm^2, 3D fluid-attenuated inversion recovery images, and 3D T2*-weighted images were obtained to assess acute infarct and hemorrhagic lesions.

CFD Analysis

One author (F.M.) who was blinded to patient information performed semiautomated segmentation of LSAs and adjacent arteries from the HR-MRA source images and then reconstructed surface models using a software package (Mimics Innovation Suite 17.0, Materialize, Belgium). After remeshing based on voxel size and a curvature smoothing method, the hybrid tetrahedral-prism numerical meshes of .3 mm in size and 5 boundary layers near the wall were generated using an octree method (ICEM CFD 14.5, ANSYS, PA).

The CFD analysis was performed using a commercial software package (ANSYS Fluent 14.5, ANSYS, PA) under a 3 cycle pulsatile flow condition[13] and calculated WSS, WSS gradient (WSSG), and flow velocity (FV) maps using the parameters as follows: the blood density/viscosity, 1056 kg/m^3/.0035 Pa·s; the outlet, time-independent and 0 Pa; and the wall, time-independent, no-slip, and rigid. The same operator semiautomatically generated regions-of-interest of LSAs and M1 using a software package (AVS 8.3, Cybernet Systems, Japan) and then obtained average WSS, WSSG, and FV values within the regions-of-interests.

Image Analysis

Two board certified neuroradiologists (T.H. and M.S.), who were blind to subject information, visually assessed whether the infarcts were located in the LSA territory or in the territories of other arteries, such as the anterior choroidal artery, thalamogeniculate artery, and long insular artery on DWI and fluid-attenuated inversion recovery images, according to a standard atlas.[14] They also assessed steno-occlusive changes of the LSAs and M1s and determined the relevant LSA that was contiguous to the infarct on MRA source images, because size and shape of the relevant artery can be altered. The visual assessments were performed 2 times with a 2-week interval. Differences between the interpretations were resolved by a consensus.

In addition, another author (F.M.) measured the maximum diameter and volume of the infarcts on DWI using a free software package (3DSlicer, www.slicer.org).[15] The maximum diameter was manually measured using a linear cursor and the volume was semiautomatically calculated with the cutoff values of −2 standard deviation of signal intensity in the infarct areas. Further, the same author measured curved and straight lengths of the LSAs on the coronal maximum intensity projection images, and calculated tortuosity by dividing the curved length by the straight length, according to the previous studies.[6,7] The measurements were performed blindly 2 times with a 2-week interval and randomized orders and were then averaged.

Statistical Analyses

The average WSS, WSSG, and FV values of the LSAs (except for the relevant LSA) and M1, straight/curved lengths and tortuosity of the LSAs, as well as the number of the LSAs were compared between the ipsilesional and contralesional sides using the Wilcoxon signed-rank test as well as between the LSA-territory and non-LSA territory groups using Mann-Whitney *U* test. The relative ipsilesional values (ipsilesional average values − contralesional average values) were also compared between the LSA-territory and non-LSA-territory groups using the Mann-Whitney *U* test. Furthermore, we examined correlations between the CFD values and the infarct volumes using Spearman's correlation coefficient. Patient characteristics were compared between the LSA infarcts and non-LSA infarcts groups using the Mann-Whitney *U* test or Fisher exact test. Intra-/inter-rater agreements were examined using kappa statistics or intraclass correlation coefficient. These statistical analyses were performed using GNU R software 3.3.0 (R Foundation) with an alpha value of .05.

Results

All patients underwent MR examination; however, 1 patient abandoned the scans due to a claustrophobic complaint. Five patients were excluded because of poor MRA images mainly due to considerable motion artifacts, which can cause substantial errors in the mesh modeling. Two patients were excluded because of substantial M1 stenosis at 7T, which can induce errors in the CFD values of LSAs; while there were no steno-occlusive changes in the LSAs except for the relevant ones. The remaining 43 patients (31 men and 12 women; 37-82 years; affect side, left/right 25/18) were eligible for further analyses. In these patients, MR examination was performed 3-21 days after onset of symptoms. The infarcts were located in the LSA territory in 29 and in the non-LSA territory in 14 (anterior choroidal artery 9, long insular artery 3, and thalamogeniculate artery 2) patients. The number of LSAs on the MRA images was 2-4 (median, 3) and 2-4 (3) in affected and nonaffected sides, respectively; while those on the surface models used for the CFD analyses were 1-4 (2) and 1-4 (2), respectively; which showed no significant laterality (P = .34-.62). There were no significant differences in the patient characteristics between the patients with LSA-territorial infarcts (LSA-territory group) and those with non-LSA territorial infarcts (non-LSA-territory group) (P = .10-.53) (Table. 1). Regarding intra/interobserver agreements, kappa values were .80/.92 and the intraclass correlation coefficient values were .82/.99, indicating good intra/inter-rater agreements.

The quantitative analyses revealed that, in the LSA-territory group, the average values of the WSS, WSSG, and FV in ipsilesional, nonrelevant LSAs (.56-5.43 Pa [median, 2.24], 9.33-107.8 × 10^4 Pa/m [30.4], and .39-5.27 cm/s [1.94], respectively) were significantly lower than those in the contralesional side (1.01-7.35 Pa [3.43], 12.5-145.7 × 10^4 Pa/m [49.0], and 1.05-8.73 cm/s [3.79], respectively) (P = .01-.03). In contrast, in the non-LSA-territory group, the CFD values of the LSAs showed no significant differences between the ipsilesional and contralesional sides (P = .39-.67). On the other hand, the CFD values of the M1 showed no significant differences between the ipsilesional and contralesional sides both in the LSA-territory and non-LSA-territory groups (P = .09-1.00) (Fig. 1,2, Table 2).

Regarding the curved length, straight length, and tortuosity of the LSAs, there were no significant differences between the ipsilesional (15.3-56.2 mm [median: 28.0], 10.6-41.4 mm [21.3], and 1.07-2.18 [1.27], respectively) and contralesional sides (16.9-51.5 mm [29.1], 14.2-38.8 mm [22.8], and 1.06-2.13 [1.29], respectively) in the LSA-territory group (P = .16-.98), as well as in the non-LSA-territory group (ipsilesional, 12.9-43.8 mm [27.3], 10.6-36.9 mm [19.8], and 1.03-1.93 [1.32], respectively; contralesional, 14.1-46.5 mm [29.8], 12.0-36.9 mm [22.1], and 1.09-1.76 [1.33], respectively; P = .25-.71).

When comparing the LSA-territory group with the non-LSA-territory group, the relative WSSG values of the ipsilesional LSAs against the contralesional ones were significantly lower in the LSA-territory group (−101.2-34.3 [−12.6]) than in the non-LSA-territory group (−44.9-21.7 [8.34]) (P= .03), while other combinations of the absolute

Table 1. *Demographics of the patients with acute infarcts of LSA and non-LSA territories*

	LSA territory infarcts (n = 29)	Non-LSA territory infarcts (n = 14)	*P*-value*
Age (years)	37-82 (66)	45-78 (64)	.46
Sex (men)	20 (69)	11 (79)	.72
NIHSS at admission	0-8 (3)	1-4 (2)	.10
Hemiplegia	22 (76)	11 (79)	1.00
Sensory disturbance	4 (14)	3 (21)	.66
Dysarthria	16 (55)	5 (36)	.33
Ataxia	5 (17)	1 (7)	.65
Hypertension	18 (62)	7 (50)	.53
Diabetes mellitus	5 (17)	6 (43)	.13
Dyslipidemia	18 (62)	6 (43)	.33
Affected side (left)	14 (48)	11 (79)	.10
MRI scan date after onset	5-19 (9)	3-21 (11.5)	.28

Abbreviations: LSA, lateral striate artery; NIHSS, National Institutes of Health Stroke Scale.
Data are presented as range (median) or number (%).
*Fisher's exact test or Mann-Whitney *U* test.

or relative values showed no significant differences (*P*= .07-.96) (Figure 2, Table 2). Regarding the relationships between the CFD metrics and the infarct size, the WSS, WSSG, and FV values in the LSA-territory group showed poor and insignificant correlations with the infarct volume (r = .12-.14).

Discussion

In this study, we successfully reconstructed precise surface models of intracranial arteries, including LSAs, from HR-MRA data at 7T in patients with acute ischemic stroke and achieved CFD measurements of WSS and related metrics of LSAs and adjacent arteries. Furthermore, we revealed that WSS, WSSG, and FV values of the LSAs in patients with LSA-territorial infarcts were significantly lower in the ipsilesional sides than in the contralesional sides, while there were no substantial differences in those of the M1s. In addition, the patients with non-LSA territorial infarcts showed no significant ipsi-/contralesional differences in the values of the LSAs and M1s. These results suggest that fluid dynamic profiles of the LSAs can be closely related with ischemic stroke confined in the LSA territory.

In general, hemodynamic shear stress to arterial walls is a crucial determinant of function and phenotype of endothelial cells, and low WSS conditions can promote progression of atherosclerosis and inflammation via endothelial dysfunction and activation of biochemical mediators.[8,16] CFD analyses have revealed that atherogenesis-susceptible locations, such as the carotid bifurcation, showed decreased WSS and related metrics.[8,9] Hence, ipsilesional LSAs with low WSS profiles were speculated to be prone to atherosclerotic and/or inflammatory changes, which may induce LSA mural lesions such as microatheroma, and eventually cause noncardioembolic infarcts in the LSA territory. On the other hand, it remains unclear whether the CFD metrics are related to lipohyalinosis of distal LSAs, which is known to be induced by hypertension. CFD analyses for patients with cerebral small vessel disease may provide some information regarding this issue. Branch atheromatous disease , ie, steno-occlusive changes at the origin of a perforating artery due to a junctional plaque, is said to be another possible mechanism to cause LSA territorial infarcts.[17] In this study, however, there were no lateralities in the CFD metrics of the M1 and there were no patients with occlusion or stenosis at the LSA origin. Hence, relationships between CFD metrics and branch atheromatous disease mechanisms remain unknown.

There are several morphological characteristics in the LSAs. The LSAs originate mainly from M1 with perpendicular or reverse directions and form S-shaped loops before piercing the anterior perforated substance[4] and become remarkable in elderly and hypertensive individuals.[6,7] Previous reports revealed that the number and length of the LSAs tended to be lower in patients with hypertension and chronic infarction as compared with healthy individuals.[6,7,18] These features may affect the results of CFD analyses because WSS and related metrics substantially depend on morphological features of the target vessels. However, the number, length, and tortuosity of the LSAs showed no significant differences between the ipsilesional and contralesional sides according to the results of this study. Hence, the laterality of the CFD metrics that we demonstrated only in the LSA-territorial group is considered to reflect fluid dynamic characteristics that can induce LSA-territorial infarcts presumably through microatheroma and/or inflammation, which cannot be revealed by morphological findings of the LSAs.

We performed CFD analyses of normal-appearing LSAs and adjacent arteries. There have been few CFD studies

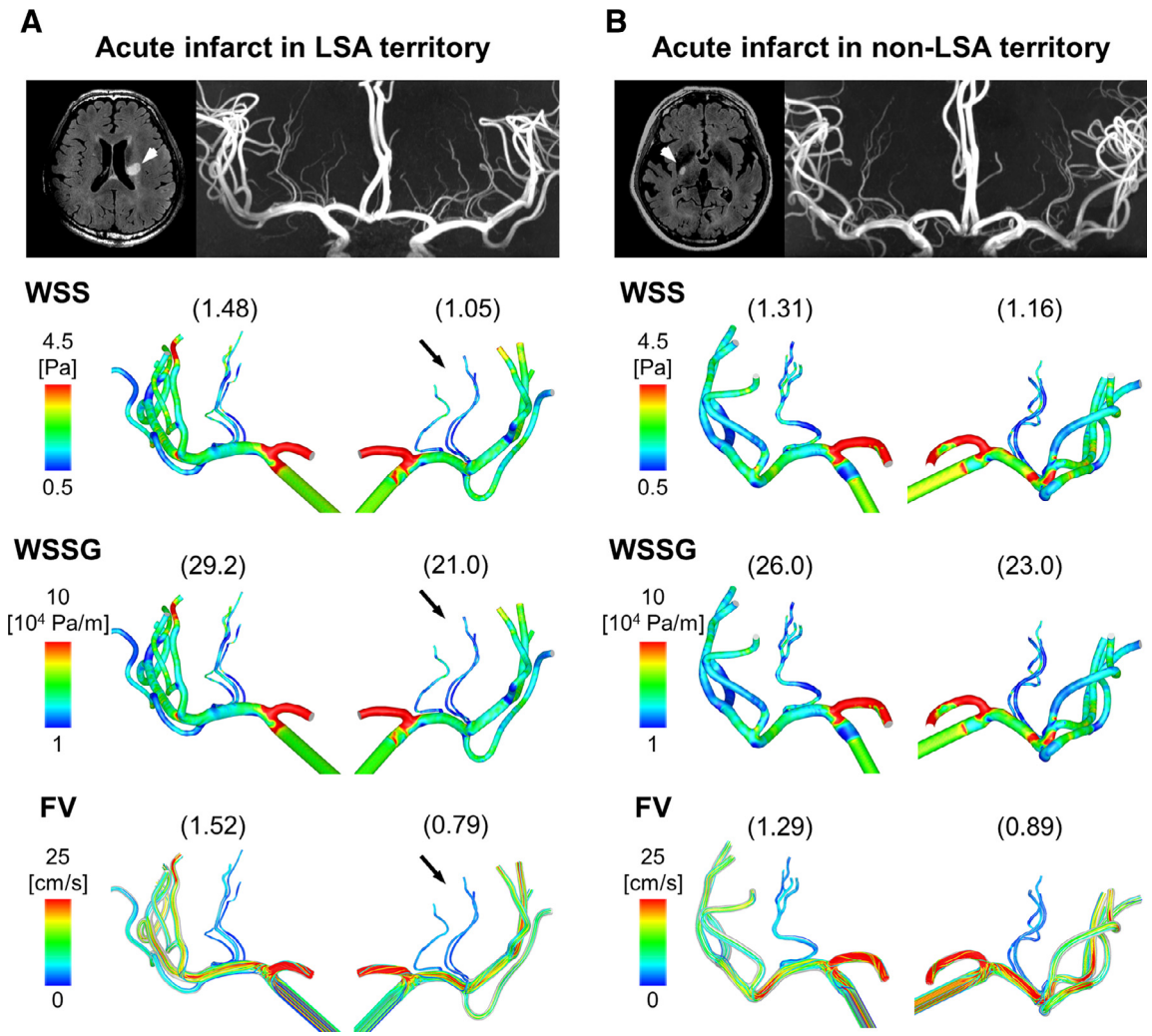

Figure 1. *CFD metrics of LSAs and adjacent intracranial arteries in patients with infarcts of LSA and non-LSA territories (A) A 68-year-old woman with acute infarct in the LSA territory (10 days after onset). A hyperintensity lesion is found in the left corona radiata and the body of the caudate nucleus on the FLAIR image (arrowhead); however, there are no apparent lesions in the intracranial arteries on MRA. Wall shear stress (WSS), WSS gradient (WSSG), and flow velocity (FV) values of the LSAs appear lower in the ipsilesional side than in the contralesional side (arrows and parentheses), while those of the M1s show no apparent laterality. (B) A 62-years-old man with acute infarct in the non-LSA territory (12 days after onset). A hyperintensity lesion is located in the posterior limb of the right internal capsule (arrowhead), while there are no apparent arterial lesions on MRA. The CFD metrics values showed no apparent laterality in the LSAs and M1s. Abbreviations: CFD, computational fluid dynamics; FLAIR, fluid-attenuated inversion recovery; LSA, lateral striate artery; M1, horizontal portion of middle cerebral artery; parenthesis (value of CFD metrics).*

regarding apparently normal intracranial arteries, although CFD profiles of stenotic major arteries have been thoroughly investigated.[19] In this study, there was significant laterality in CFD metrics of normal-appearing LSAs in patients with LSA-territorial infarcts, suggesting that CFD analysis of normal intracranial arteries can provide additional information regarding the pathogenesis of ischemic stroke. Besides CFD analysis, advanced imaging techniques such as time-resolved rotational angiography have been used to obtain flow information of the LSAs.[5,19] However, these techniques cannot obtain WSS or WSSG, which show changes that are more significant than FV in this study. Hence, CFD measurements of the WSS and related metrics appear effective to assess infarct-susceptible characteristics of normal-appearing intracranial arteries, including the LSAs.

This study had several limitations. First, we performed comparisons between ipsi- and contralesional sides of infarcts and between infarcts of the LSA and non-LSA territories but not between the stroke patients and age-matched healthy individuals, because subjects' background such as existence of hypertension and dyslipidemia can cause morphological changes of intracranial arteries, which can be substantial biases for CFD analyses. Hence, it remains unknown whether the CFD metrics values of the ipsilesional or contralesional LSAs in stroke patients are lower or higher than those in control subjects. In addition, we cannot determine whether the values of

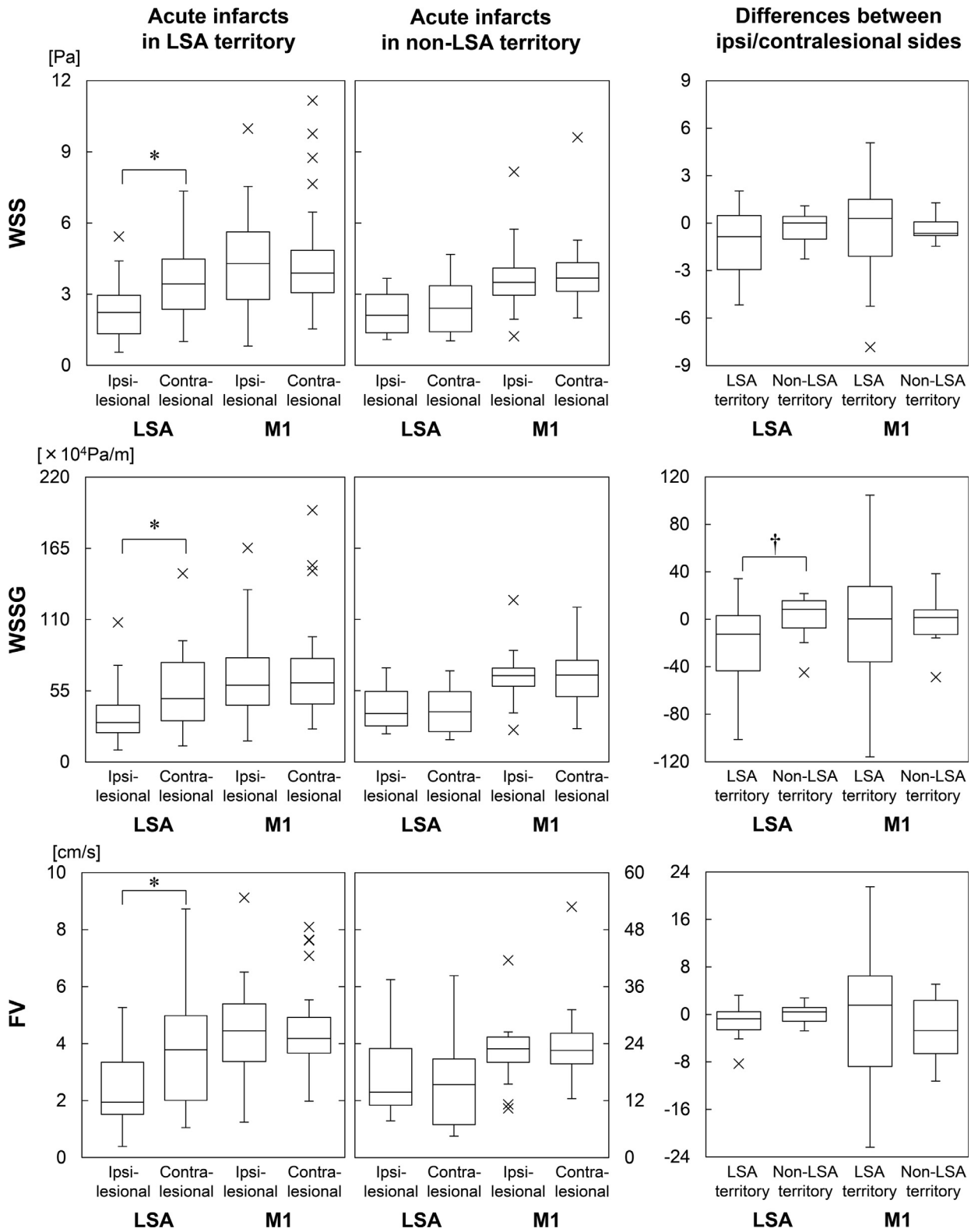

Figure 2. *Absolute and relative values of CFD metrics in the LSAs and M1s of patients with infarcts of LSA and non-LSA territories. WSS, WSSG, and FV values of the LSAs are significantly lower in the ipsilesional side than in the contralesional side only in patients with LSA-territorial infarcts. Relative WSSG values (ipsilesional minus contralesional) are significantly lower in patients with LSA territorial infarcts than those with non-LSA territorial infarcts. There are no significant differences in other combinations. * Wilcoxon signed-rank test, †Mann-Whitney U test. Abbreviations: CFD, computational fluid dynamics; FV, flow velocity; LSA, lateral striate artery; WSS, wall shear stress; WSSG, wall shear stress gradient.*

Table 2. *CFD metrics of LSAs and M1 in patients with infarcts of LSA and non-LSA territories*

	CFD metrics	Absolute values						Relative values (ipsilateral minus contralateral)		
		LSA territory infarcts (n = 29)			Non-LSA territory infarcts (n = 14)			LSA territory infarcts	non-LSA territory infarcts	*P*-value†
		Ipsilesional	Contralesional	*P*-value*	Ipsilesional	Contralesional	*P*-value*			
LSAs	WSS (Pa)	.56-5.43 (2.24)	1.01-7.35 (3.43)	**.02**	1.09-3.67 (2.11)	1.04-4.67 (2.41)	.63	−5.17-2.03 (−.85)	−2.26-1.09 (.01)	.30
	WSSG ($\times 10^4$ Pa/m)	9.33-107.8 (30.4)	12.5-145.7 (49.0)	**.01**	21.6-72.6 (37.3)	17.2-70.4 (38.7)	.39	−101.2-34.3 (−12.6)	−44.9-21.7 (8.34)	**.03**
	FV (cm/s)	.39-5.27 (1.94)	1.05-8.73 (3.79)	**.03**	1.29-6.25 (2.30)	.75-6.39 (2.56)	.67	−8.31-3.23 (−.74)	−2.75-2.78 (.42)	.05
M1	WSS (Pa)	.82-9.98 (4.29)	1.54-11.2 (3.89)	.94	1.24-8.16 (3.50)	2.00-8.16 (3.72)	.09	−7.83-5.08 (.30)	−1.45-1.29 (−.64)	.48
	WSSG ($\times 10^4$ Pa/m)	16.4-165.4 (59.3)	25.5-194.5 (61.1)	.90	24.6-124.9 (66.6)	25.7-119.5 (67.0)	1.00	−115.9-104.6 (.36)	−48.8-38.5 (1.51)	.94
	FV (cm/s)	7.41-54.7 (26.7)	11.8-48.6 (25.1)	.97	10.2-41.4 (22.8)	12.2-52.7 (22.4)	.22	−22.4-21.5 (1.55)	−11.3-5.09 (−2.72)	.52

Abbreviations: CFD, computational fluid dynamics; FV, flow velocity; LSA, lateral striate artery; M1, horizontal portion of middle cerebral artery; WSS, wall shear stress; WSSG, wall shear stress gradient.

The significance of bold shows significant difference.

Data are presented as range (median).

*Wilcoxon signed-rank test.

†Mann-Whitney *U*-test.

the ipsi/contralesional LSAs in the LSA-territorial infarcts are lower/higher than those in the non-LSA territorial infarcts, because there were no significant differences between the groups. Second, we were only able to enroll a relatively small number of patients, mainly because of the strict exclusion criteria. Further, several patients were ineligible for the surface modeling due to marked motion artifacts of HR-MRA that require a long acquisition time. These patient-related issues could have affected the results of this study. Third, we were able to generate surface models of only 1-4 of the LSAs and had to ignore the more distal parts of the LSAs because of limited spatial resolution of the HR-MRA. These issues also may influence the results. MRA with higher spatial resolution is needed to include more LSAs for CFD analyses. Rotational angiography[5] or high-resolution computed tomography angiography[18] can be other candidates of source images for this purpose. Finally, there are technical issues regarding CFD analyses. We used fixed boundary conditions for the CFD analyses as the previous CFD studies of intracranial arteries. However, subject-specific conditions such as blood pressure and hematocrit have been reported to affect the results.[20] The usage of the boundary conditions obtained by the patient-specific measurement value may further improve accuracies of the CFD metrics.

In conclusion, CFD analyses of the LSAs using HR-MRA at 7T revealed that WSS, WSSG, and FV values were significantly lower in the ipsilesional LSAs in patients with LSA-territory infarcts, suggesting that fluid dynamic characteristics of the LSAs can be related to the pathogenesis of ischemic stroke confined in the LSA territory.

Author's Contributions

F.M.: Project development, Data analysis, Manuscript writing; F.I.: Data analysis, Technical support; T.N.: Data collection; H.M.: Data collection; H.K.: Data collection; T.H.: Data analysis; K.Y.: Helped manuscript writing; F.Y.: Helped data analysis; I.U.: Helped data analysis; K.I.: Helped data analysis; M.S.: Project development, Data analysis, Helped manuscript writing.

Declaration of Competing Interest

The authors declare no competing interests.

References

1. Rovira A, Grive E, Rovira A, et al. Distribution territories and causative mechanisms of ischemic stroke. Eur Radiol 2005;15:416-426.
2. Norrving B. Long-term prognosis after lacunar infarction. Lancet Neurol 2003;2:238-245.
3. Arboix A, Marti-Vilalta JL. Lacunar stroke. Expert Rev Neurother 2009;9:179-196.
4. Marinkovic S, Gibo H, Milisavljevic M, et al. Anatomic and clinical correlations of the lenticulostriate arteries. Clin Anat 2001;14:190-195.
5. Kammerer S, Mueller-Eschner M, Berkefeld J, et al. Time-resolved 3d rotational angiography (4d dsa) of the lenticulostriate arteries: display of normal anatomic variants and collaterals in cases with chronic obstruction of the MCA. Clin Neuroradiol 2017;27:451-457.
6. Kang CK, Park CA, Lee H, et al. Hypertension correlates with lenticulostriate arteries visualized by 7T magnetic resonance angiography. Hypertension 2009;54:1050-1056.
7. Kang CK, Park CA, Park CW, et al. Lenticulostriate arteries in chronic stroke patients visualised by 7T magnetic resonance angiography. Int J Stroke 2010;5:374-380.
8. Malek AM, Alper SL, Izumo S. Hemodynamic shear stress and its role in atherosclerosis. JAMA 1999;282:2035-2042.
9. Cheng C, Tempel D, van Haperen R, et al. Atherosclerotic lesion size and vulnerability are determined by patterns of fluid shear stress. Circulation 2006;113:2744-2753.
10. Peiffer V, Sherwin SJ, Weinberg PD. Does low and oscillatory wall shear stress correlate spatially with early atherosclerosis? A systematic review. Cardiovasc Res 2013;99:242-250.
11. Zhou G, Zhu Y, Yin Y, et al. Association of wall shear stress with intracranial aneurysm rupture: systematic review and meta-analysis. Sci Rep 2017;7:5331.
12. Ojha M. Wall shear stress temporal gradient and anastomotic intimal hyperplasia. Circ Res 1994;74:1227-1231.
13. Ford MD, Alperin N, Lee SH, et al. Characterization of volumetric flow rate waveforms in the normal internal carotid and vertebral arteries. Physiol Meas 2005;26:477-488.
14. Tatu L, Moulin T, Bogousslavsky J, et al. Arterial territories of the human brain: cerebral hemispheres. Neurology 1998;50:1699-1708.
15. Fedorov A, Beichel R, Kalpathy-Cramer J, et al. 3D slicer as an image computing platform for the quantitative imaging network. Magn Reson Imaging 2012;30:1323-1341.
16. Hahn C, Schwartz MA. Mechanotransduction in vascular physiology and atherogenesis. Nat Rev Mol Cell Biol 2009;10:53-62.
17. Petrone L, Nannoni S, Del Bene A, et al. Branch atheromatous disease: a clinically meaningful, yet unproven concept. Cerebrovasc Dis 2016;41:87-95.
18. Gotoh K, Okada T, Satogami N, et al. Evaluation of CT angiography for visualisation of the lenticulostriate artery: difference between normotensive and hypertensive patients. Br J Radiol 2012;85:e1004-e1008.
19. Liu J, Yan Z, Pu Y, et al. Functional assessment of cerebral artery stenosis: a pilot study based on computational fluid dynamics. J Cereb Blood Flow Metab 2017;37:2567-2576.
20. Nam HS, Scalzo F, Leng X, et al. Hemodynamic impact of systolic blood pressure and hematocrit calculated by computational fluid dynamics in patients with intracranial atherosclerosis. J Neuroimaging 2016;26:331-338.